Available online at www.sciencedirect.com

ScienceDirect

Ceramics International 40 (2014) 5033–5038

CERAMICS INTERNATIONAL

www.elsevier.com/locate/ceramint

Short communication

Properties of novel $Li_{4-3x}Cr_xSiO_4$ ceramic electrolyte

S.B.R.S Adnan[a], N.S. Mohamed[b,*]

[a]Institute of Graduate Studies, University of Malaya, 50603 Kuala Lumpur, Malaysia
[b]Centre for Foundation Studies in Science, University of Malaya, 50603 Kuala Lumpur, Malaysia

Received 11 July 2013; received in revised form 29 August 2013; accepted 29 August 2013
Available online 8 September 2013

Abstract

Cr-doped Li_4SiO_4 compounds were prepared by a sol–gel method. The effects of Cr^{3+} doping on the characteristics of Li_4SiO_4 were carefully investigated. Compared with the XRD pattern of the Li_4SiO_4 sample, the XRD patterns of the Cr-doped Li_4SiO_4 shift to higher diffraction angle. This indicated that Cr^{3+} entered the structure of Li_4SiO_4 rather than forming impurities. The formation of the compound was confirmed by Fourier transform infrared study. The introduction of Cr^{3+} ions considerably raised the conductivity of the Li_4SiO_4 compound. The compound of $Li_{3.94}Cr_{0.02}SiO_4$ exhibited total conductivity value of 2.51×10^{-5} S cm^{-1} at ambient temperature and 5.69×10^{-4} S cm^{-1} at 500 °C. Ionic transference number corresponding to Li^+ ion transport determined by means of Bruce and Vincent technique was 0.95. Linear sweep voltammetry result showed that the doping of Cr^{3+} ion improved the limit of electrolyte decomposition to 4.51 V versus a Li/Li^+ reference electrode.

Keywords: C. Ionic conductivity; Lithium orthosilicate; Linear sweep voltammetry; Solid electrolyte

1. Introduction

Lithium super ionic conductor (LISICON) is one of promising groups of crystalline materials that is very important for future application as solid electrolyte in lithium batteries. This type of electrolytes is considered to be effective in improving the safety of lithium ion batteries compared to the traditional liquid electrolyte. Among solid electrolytes, the application of ceramic electrolytes form an important class of materials due to their large electrochemical stability window, good thermal stability, absence of leakage and a high resistance to shock and vibrations. Meanwhile, the use of ceramic materials in electrochemical devices can also solve the problem of capacity fading and self discharge cause by side reactions [1]. Many attempts to synthesize new ceramic lithium superionic conductors have been made. The highest conductivity of 10^{-3} S cm^{-1} was previously reported for the thio-LISICON structure, $Li_{3.25}Ge_{0.25}P_{0.75}S_4$ [2]. However this type of materials has disadvantages such as complicated to prepare, toxic, show instability against electrochemical reduction at low potential (ca. 0.1 V versus Li/Li^+), and also exhibits incompatibility with graphite anode [3].

In the search of fast lithium conducting solid electrolyte, the authors found recently new solid solution systems based on the lithium orthosilicate, Li_4SiO_4. These compounds with the general formula, $Li_{4-3x}Cr_xSiO_4$, are isostructural with γ-Li_3PO_4 and have the same framework structure with the thio-LISICON. However, the thio-LISICON structure have sulfur instead of oxygen in this structure. The substitution of Li with Cr ($3Li^+ \leftrightarrow Cr^{3+}$) will create two vacant sites in the structure and any lithium ion in the intermediate vicinity can jump to the vacant sites. This leaves the previous two sites of the ion vacant available to host other ions. This results in the mobility of ions across the solid giving rise the conductivity. Their concentration is the main factor determining the conductivity of this solid electrolyte [4].

Chavarria et al. [5] have previously reported conductivity data for the $Li_{4-3x}(Al,Ga,In)_xSiO_4$ at 127 °C with conductivity value 6×10^{-5} S cm^{-1} (Al system), 6×10^{-6} S cm^{-1} (Ga system) and 6×10^{-8} S cm^{-1} (In system). However, study on lithium orthosilicate doped with Cr^{3+} ions has never been reported in the literature. This doping is expected to be successful since the ion radius difference between Cr^{3+} (0.64 Å) and Li^+ (0.69 Å) is just 7.5% and does not exceed the solubility limit for atomic radii differences in solid solution which is 15% [6].

*Corresponding author. Tel.: +60 379675800.
E-mail addresses: syed_bahari@yahoo.com (S.B.R. Adnan), nsabirin@um.edu.my (N.S. Mohamed).

0272-8842/$ - see front matter © 2013 Elsevier Ltd and Techna Group S.r.l. All rights reserved.
http://dx.doi.org/10.1016/j.ceramint.2013.08.136

In this study, $Li_{4-3x}Cr_xSiO_4$ (x=0, 0.01, 0.02 and 0.03) compounds were synthesized and characterized. The effects of Cr^{3+} substitution on the properties of Li_4SiO_4 were investigated using x-ray diffraction (XRD), Fourier transform infrared (FTIR), Scanning electron microscope (SEM), Particle size analysis, impedance spectroscopy (IS), lithium transference number measurement and linear sweep voltammetry (LSV).

2. Experimental procedure

2.1. Synthesis of $Li_{4-3x}Cr_xSiO_4$

For this study, four compounds with x=0, 0.01, 0.02 and 0.03 were prepared via sol–gel technique. For sample preparation, lithium acetate, chromium (III) acetate hydroxide and tetraethyl orthosilicate were used as the starting materials. Meanwhile citric acid was used as the chelating agent. The molar ratio of Li:Cr:Si was fixed according to formula $Li_{4-3x}Cr_xSiO_4$ with x=0, 0.01, 0.02 and 0.03. Lithium acetate and chromium (III) acetate hydroxide were first dissolved in distilled water and then mixed with citric acid under magnetic stirring. The solution was transferred into a reflux system and continuously stirred until a homogeneous solution was formed. Solution of tetraethyl orthosilicate was later added to this homogeneous solution. After stirring for 12 h, the solution was taken out and then vaporized for about 2 h under magnetic stirring at 75 °C. The resulting sticky wet gel was dried in an oven at 150 °C for 24 h. The obtained powder was ball milled for 24 h using a Fritsch Pulverisette-7 ball mill operated at 500 rpm. The powder was sintered at temperature 800 °C for 12 h and later pressed using a Specac pellet press to form pellet with diameter and thickness of 13 mm and 2.0 mm respectively.

2.2. Characterization techniques

XRD patterns of the powder samples were obtained using X-ray Diffraction spectrometer (Bruker AXS D8 Advance) with Cu-K_α radiation of wavelength of 1.5406 Å in 2θ range between 10° and 70° at the rate of 0.016° in step width. FTIR was carried out to confirm the structure of the studied ceramic samples. Infrared spectra were recorded at room temperature using a Perkin-Elmer Frontier Spectrometer with resolution 1 cm^{-1}. The absorption spectra in FIR region were measured using polyethylene technique. The morphology of the sample powders were analyzed by SEM which were carried out using Scanning electron microscope spectrometer (Zeiss-Evo MA10). The particle size information was obtained using FRITSCH-Analysette 22 NanoTec laser particle sizer. The ceramic electrical properties were determined by ac impedance spectroscopy using Solatron 1260 impedance analyzer over a frequency range from 1 to 10^6 Hz. An applied voltage was fixed at 200 mV.

Lithium transference number measurement was done using Bruce and Vincent method [7–9] in order to determine the actual type of charge carriers. The lithium transference number (τ_{Li}^{+}) was calculated using the equation:

$$\tau_{Li^+} = \frac{I_{ss}(\Delta V - I_o R_o)}{I_o(\Delta V - I_{ss} R_{ss})} \quad (1)$$

In this equation, I_o is initial current (t=0), I_{ss} is steady state current, R_o and R_{ss} are initial resistance of the passive layer (before polarization) and resistance of the passive layer (after polarization) respectively and ΔV is applied voltage bias (ΔV=0.5 V). The electrochemical stability was evaluated by linear sweep voltammetry using Wonatech ZIVE MP2 multichannel electrochemical workstation.

3. Result and discussion

3.1. Phase identification

Fig. 1(a) shows XRD spectra of the monoclinic $Li_{4-3x}Cr_xSiO_4$ (x=0, 0.01, 0.02 and 0.03) samples. Cr^{3+} could be doped on the Li sites ($3Li^+ \leftrightarrow Cr^{3+}$) with up to x=0.020 without the presence of impurities. As such, further analysis was only done on the samples with $0 < x < 0.02$. To confirm the Cr^{3+} ion is in the Li_4SiO_4 structure, the peaks in 2θ range 16.50°–17.10° were carefully analyzed. Fig. 1(b) shows the magnified XRD patterns in this 2θ range. As seen in this figure, the peak shifts to higher diffraction angle when Cr^{3+} ion is doped into the parent structure indicating that Cr^{3+} ion is in the Li_4SiO_4 structure rather than forming impurities. The diffraction peak is also broadened by

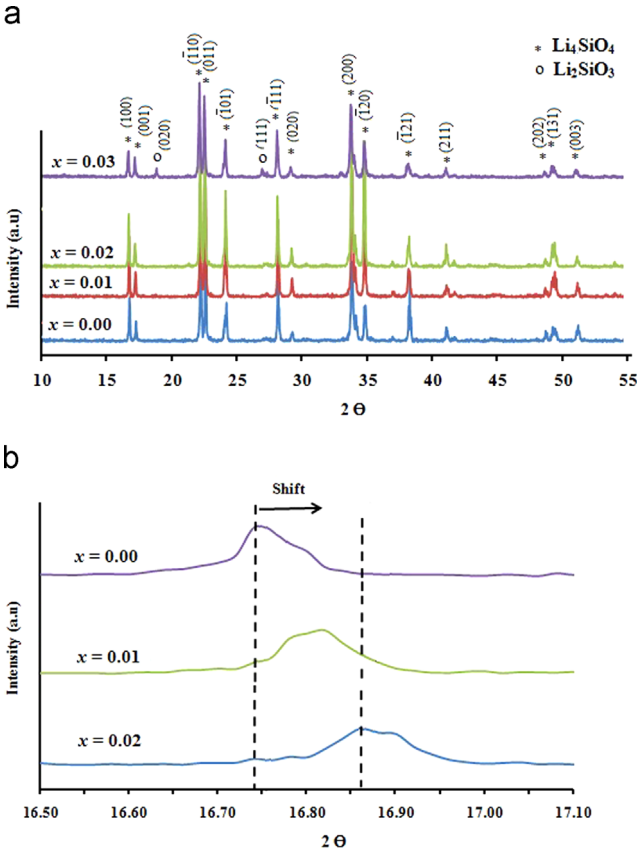

Fig. 1. (a) XRD patterns of $Li_{4-3x}Cr_xSiO_4$ samples and (b) XRD patterns of $Li_{4-3x}Cr_xSiO_4$ samples in 2θ range from 16.50° to 17.10°.

Cr^{3+} doping, which implies that the crystal size decreases with increasing Cr^{3+} content.

Meanwhile, the variation of the lattice parameters of the monoclinic γ-solid solution with different Cr^{3+} contents are shown in Table 1. Based on the table, the value of *a* increases and then decreases while the values of *b*, *c*, β and unit cell volume (*V*) decrease with increase of Cr^{3+} ion content. The decrease in the lattice constants is attributable to the substitutions of smaller volume of Cr^{3+} ion compared to three volumes of Li^{+} ions. The substitution of lithium by Cr^{3+} which results in shrinkage of unit cell volume increases the stability of the compound's structure [10].

3.2. FTIR analysis

Fig. 2 presents the FTIR spectra for $Li_{4-3x}Cr_xSiO_4$ samples in the spectral region from 460 cm^{-1} and 500 cm^{-1} which corresponds to absorption peaks originated from Li–O and Li–O–Si groups [11–13]. The increasing of Cr^{3+} concentration results in a decrease in intensity of the peaks. This effect is due to the coordination of the cation of Cr^{3+} with the oxygen, which results in the weakening of the Li–O and Li–O–Si and change in the lattice parameters as mentioned earlier.

3.3. SEM and particle size distribution

The SEM micrographs and particle size distribution of $Li_{4-3x}Cr_xSiO_4$ ceramic powders are displayed in Fig. 3. From these images, it is clear that the particle size decreases with increasing Cr^{3+} content. The average grain size decreases from 11.8 μm in the Li_4SiO_4 sample to 0.59 μm in the $Li_{3.94}Cr_{0.02}SiO_4$ sample. The smaller particles in $Li_{3.940}Cr_{0.020}SiO_4$ is favorable as this may improve contact with electrode materials when it is used for device fabrication.

3.4. Impedance measurement

Impedance spectra for $Li_{4-3x}Cr_xSiO_4$ with $x=0$, 0.01 and 0.02 at ambient temperature are presented in Fig. 4. The figure shows a high and low frequency semicircle for all samples. The total conductivity, (σ_t) (bulk conductivity, σ_b+grain boundary conductivity, σ_{gb}) which represent the direct current (d.c) conductivity in the ceramic sample can be calculated from equation [14]:

$$\frac{1}{\sigma_t} = \frac{1}{\sigma_b} + \frac{1}{\sigma_{gb}} \tag{2}$$

where $\sigma_b = d/AR_b$ and $\sigma_{gb} = d/AR_{gb}$. In these equation, *d* is the sample thickness, *A* is the cross-sectional area of sample, R_b is the bulk resistance and R_{gb} is the grain boundary resistance. As the Cr^{3+} concentration increases, the total resistance, $R_t = (R_b + R_{gb})$ value shifts towards lower values indicating increase in conductivity.

Fig. 5 depicts the plots of temperature dependence of total conductivity for all samples. The conductivity plots of the three samples are linear and fit the Arrhenius equation as expressed by:

$$\sigma_b T = A \exp\left(\frac{-E_\alpha}{kT}\right) \tag{3}$$

where *A* is the pre-exponential factor, E_α is the activation energy for conduction and *k* is the Boltzman constant. The conductivity of the samples increases with temperature and with Cr^{3+} ion concentration as well. The $Li_{3.94}Cr_{0.02}SiO_4$ compound gives the highest conductivity value of 2.51×10^{-5} S cm^{-1} at ambient temperature and 5.69×10^{-4} S cm^{-1} at 500 °C. The conductivity value at ambient temperature for $Li_{3.94}Cr_{0.02}SiO_4$ is an order of magnitude higher compared to the Li_4SiO_4. The σ-1000/T plots show a discontinuity at 300 °C (1000/T = 1.75 K^{-1}) which is in agreement with the results reported by Wakihara et al. [15] and those obtained by the author earlier [16]. The change in slope of the σ-1000/T plots could be due to an order-disorder transition of Li^{+} and Cr^{3+} ions (change in structure arrangement). This is support by the authors' previous work in which no phase transition was observed in the sample upon heating from room temperature until 500 °C [16].

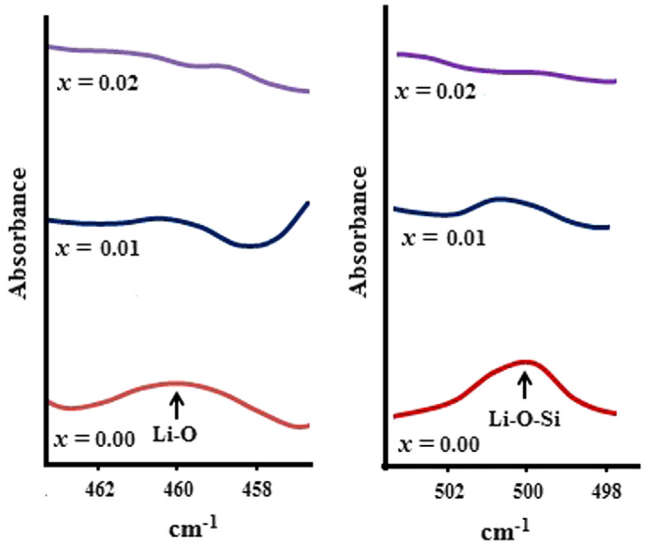

Fig. 2. FTIR spectra of $Li_{4-3x}Cr_xSiO_4$ samples in the spectral region from 458 to 462 cm^{-1} and 498 to 502 cm^{-1}.

Table 1
Lattice parameters and unit cell volume for different *x* value.

Samples	$a \pm 0.066$ (Å)	$b \pm 0.008$ (Å)	$c \pm 0.105$ (Å)	$\beta \pm 0.04$ (°)	*V* (Å^3)
$x=0.00$	5.147	6.094	5.293	90.33	166.01
$x=0.01$	5.271	6.089	5.124	90.32	164.44
$x=0.02$	5.249	6.079	5.100	90.25	162.74

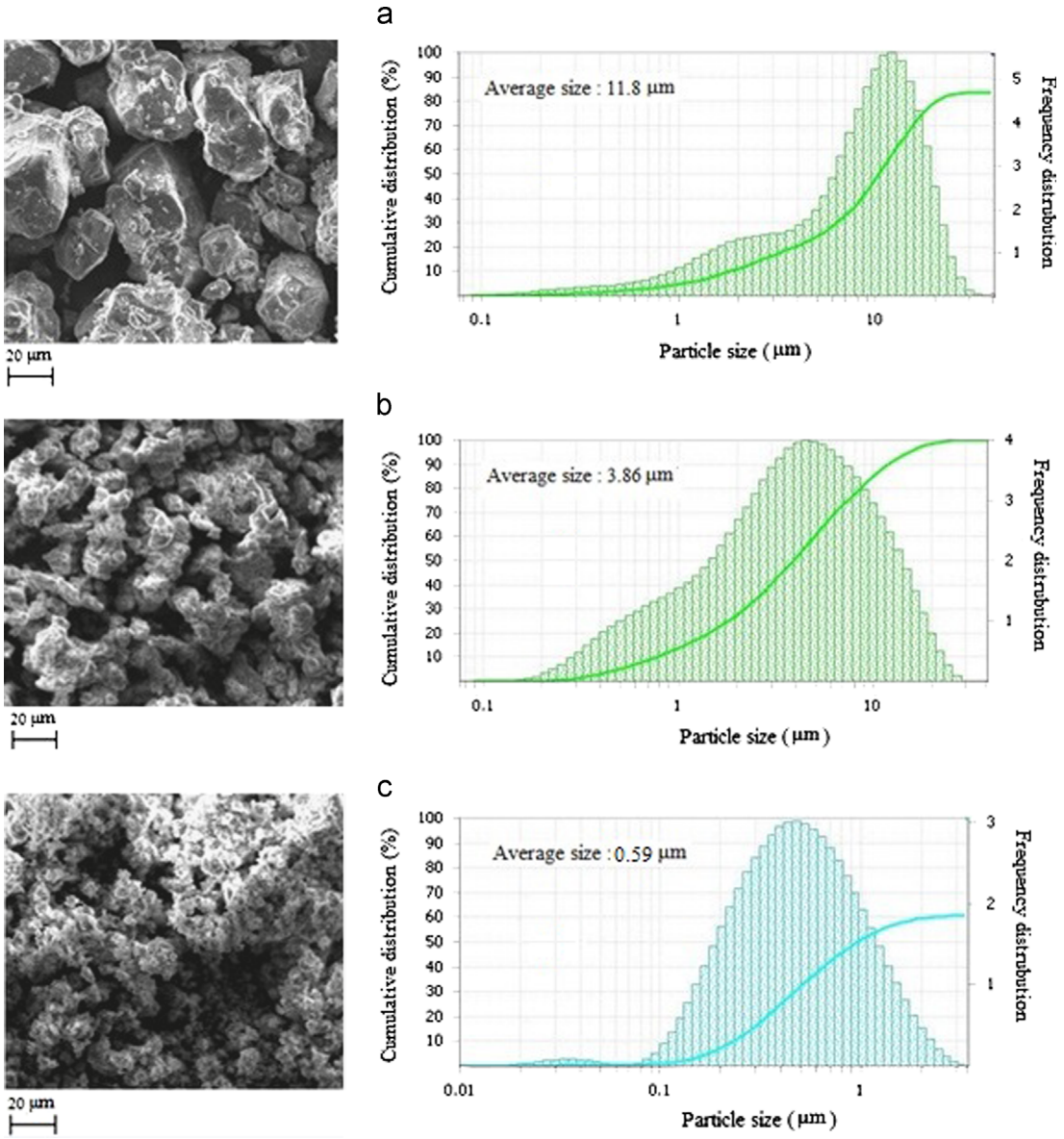

Fig. 3. SEM micrograph and particle size distribution of the (a) Li_4SiO_4 (b) $Li_{3.97}Cr_{0.01}SiO_4$ and (c) $Li_{3.940}Cr_{0.02}SiO_4$ sample.

3.5. Lithium transference number

Fig. 6(a) and (b) present plots of current versus time for the Li/$Li_{3.94}Cr_{0.02}SiO_4$/Li and Li/Li_4SiO_4/Li cells used for the lithium transference number determination of the solid electrolyte. Under a dc polarization of 0.5 V, the current in the both cells exhibit only a small decay with time. The initial and final steady current in Li/$Li_{3.94}Cr_{0.02}SiO_4$/Li cell are $I_o = 0.92$ μA and $I_{ss} = 0.87$ μA respectively. Meanwhile, the initial and final steady currents in Li/Li_4SiO_4/Li cell are $I_o = 1.67$ μA and $I_{ss} = 1.34$ μA respectively. The impedance responses of the cells prior and after polarization for Li/$Li_{3.94}Cr_{0.02}SiO_4$/Li cell are $R_o = 15{,}180$ Ω and $R_{ss} = 15{,}923$ Ω respectively. Meanwhile in Li/Li_4SiO_4/Li cell, the impedance responses prior and after polarization are $R_o = 36{,}307$ Ω and $R_{ss} = 42{,}405$ Ω respectively.

Calculation of Li^+ transference number was done using Eq. (1). The lithium transference number value is 0.95 for the $Li_{3.94}Cr_{0.02}SiO_4$ electrolyte sample and 0.79 for the Li_4SiO_4 electrolyte sample. These values show that the Cr^{3+} doping into the Li sites ($Cr^{3+} \leftrightarrow 3Li^+$) increases the Li^+ ions transport number.

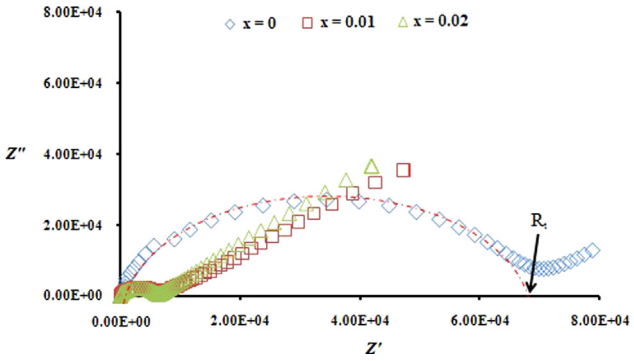

Fig. 4. The impedance spectra of $Li_{4-3x}Cr_xSiO_4$ sample.

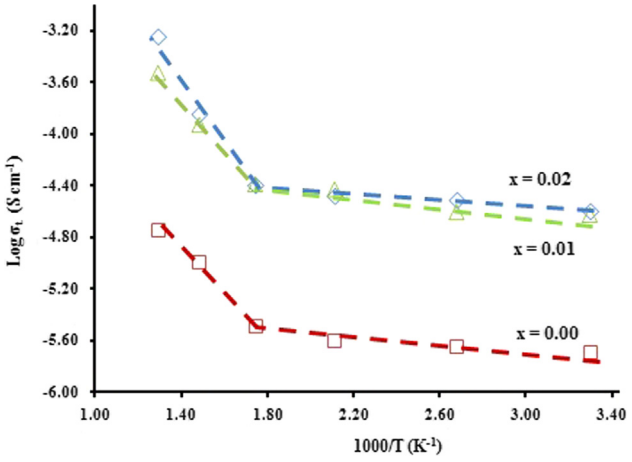

Fig. 5. Temperature dependence of total conductivity for $Li_{3.940}Cr_{0.020}SiO_4$ sample.

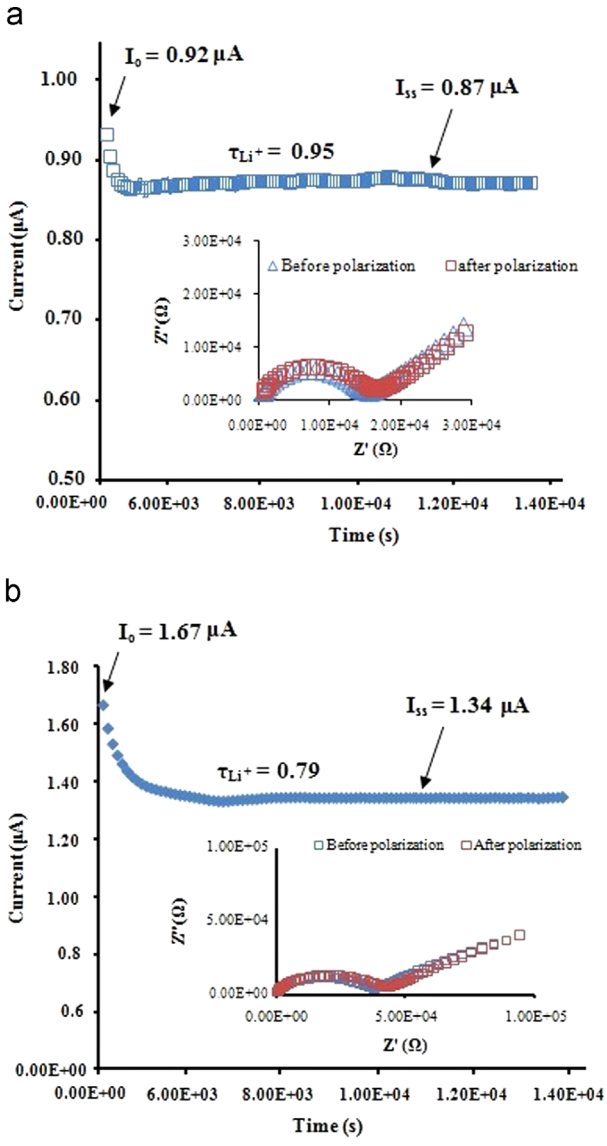

Fig. 6. (a) Current versus time plot for $Li_{3.940}Cr_{0.020}SiO_4$ sample and impedance responses of the sample before and after polarization. (b) Current versus time plot for Li_4SiO_4 sample and its impedance spectra performed before and after cell polarization are shown in inset.

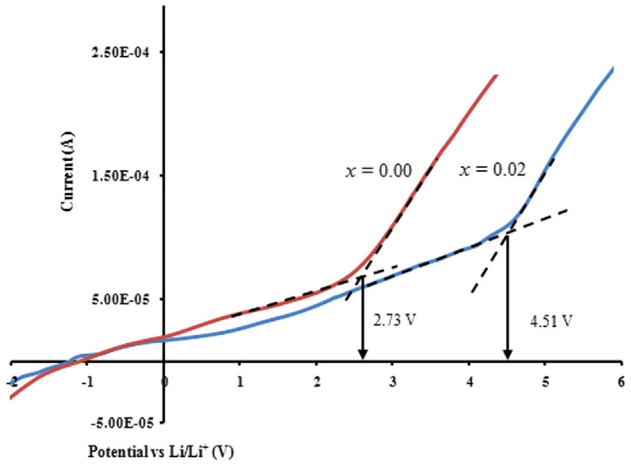

Fig. 7. Linear sweep voltammogram of Li_4SiO_4 and $Li_{3.940}Cr_{0.020}SiO_4$ at a sweep rate of 1 mV s^{-1}.

3.6. Linear sweep voltammetry

The electrochemical stability window is another important parameter of the ceramic electrolyte. The stability was evaluated by linear sweep voltammetry. Fig. 7 illustrates linear sweep voltammograms of the $Li_4Sn_{0.02}Si_{0.98}O_4$ and Li_4SiO_4 ceramic electrolyte. From the figure, the magnitude of current is fairly low below 2.73 V for Li_4SiO_4 and is 4.51 V for $Li_{3.94}Cr_{0.02}SiO_4$ respectively and the current starts increasing at potentials beyond this limit due to decomposition of the electrolyte. This suggests that the doping of Cr^{3+} ion increases the limit of electrolyte decomposition.

4. Conclusions

The effects of Cr^{3+} doping on Li_4SiO_4 were studied by XRD, FTIR, SEM, Particle size analysis, EIS, transference number and LSV. The XRD and FTIR results showed that Cr^{3+} is successfully inserted into the Li_4SiO_4 structure. The SEM showed that the grain size decreases with increase of Cr^{3+} concentration. The conductivity –temperature study illustrated that the conductivity of the compound obeys the Arrhenius law and increase with temperature. The value of lithium transference number increases upon Cr^{3+} doping. The $Li_{3.94}Cr_{0.02}SiO_4$ sample showed an increased of stable voltage window up to 4.51 V versus Li/Li^+ respectively.

Acknowledgments

Financial support from the University of Malaya (research grant PV027/2012) is gratefully acknowledged.

References

[1] B. Scrosati, Recent advances in lithium ion battery materials, Electrochimica Acta 45 (2000) 2461–2466.
[2] Masahiro Murayama, Noriyuki Sonoyama, Atsuo Yamada, Ryoji Kanno, Material design of new lithium ionic conductor, thio-LISICON, in the Li_2S–P_2S_5 system, Solid State Ionics 170 (2004) 173–180.

[3] Yuji Ooura, Nobuya Machida, Muneyuki Naito, Toshihiko Shigematsu, Electrochemical properties of the amorphous solid electrolytes in the system Li_2S–Al_2S_3–P_2S_5, Solid State Ionics 225 (2012) 350–353.
[4] P. Padma Kumar, S. Yashonathl, Ionic conduction in the solid state, Journal of Chemical Sciences 118 (2006) 135–154.
[5] J.B. Chavarria, P. Quintana, A. Huanosta, Electrical properties of the solid solution $Li_{4-3x}In_xSiO_4$, Solid State Ionics 83 (1996) 245–248.
[6] Zhanqiang Liu, Fuqiang Huang, Jianhua Yang, Baofeng Wang, Junkang Sun, New lithium ion conductor, thio-LISICON lithium zirconium sulfide system, Solid State Ionics 179 (2008) 1714–1716.
[7] P.G. Bruce, J. Evans, C.A. Vincent, Conductivity and transference number measurements on polymer electrolytes, Solid State Ionics 28-30 (1998) 918–922.
[8] M. Riley, S.Peter Fedkiw, S.A. Khan, Transport Properties of Lithium Hectorite-Based Composite Electrolytes, Electrochemical Society 149 (2002) A667–A674.
[9] A.M.M. Ali, M.Z.A Yahya, H. Nahron, R.H.Y. Subban, Electrochemical studies on polymer electrolytes based on poly(methyl methacrylate)-grafted natural rubber for lithium polymer battery, Ionics 12 (2006) 303–307.
[10] Li Fang Jiao, Ming Zhang, Hua Tang Yuan, Ming Zhao, Jian Guo, Wei Wang, Xing Di Zhou, Yong Mei Wang, Effect of Cr doping on the structural, electrochemical properties of $Li[Li_{0.2}Ni_{0.2-x/2}Mn_{0.6-x/2}Cr_x]O_2$ ($x=0$, 0.02, 0.04, 0.06, 0.08) as cathode materials for lithium secondary batteries, Journal of Power Sources 167 (2007) 178–184.
[11] Marek Nocun, Miroslaw Handke, Identification of Li–O absorption bands based on lithium isotope substitutions, Journal of Molecular Structure 596 (2001) 145–149.
[12] J. Ortiz-Landerosa, L. Martínez-dlCruz, C. Gómez-Yáñez, H. Pfeiffer, Towards understanding the thermoanalysis of water sorption on lithium orthosilicate (Li_4SiO_4), Thermochimica Acta 515 (2011) 73–78.
[13] Bo Zhang, Michel Nieuwoudt, allan J. Easteal, Sol–gel route to nanocrystalline lithium metasilicate particles, Journal of the American Ceramic Society 91 (2008) 1927–1932.
[14] Shiqiang (Rob) Hui, Justin Roller, Sing Yick, Xinge Zhang, Cyrille Decès-Petit, Yongsong Xie, Radenka Maric, Dave Ghosh, A brief review of the ionic conductivity enhancement for selected oxide electrolytes, Journal of Power Sources 172 (2007) 493–502.
[15] M. Wakihara, T. Uchida, T. Gohara, Ionic conductivity of $Li_{4-2x}Mg_{x}$-SiO_4, Solid state Ionics 31 (1988) 17–20.
[16] S.B.R.S Adnan, N.S. Mohamed, Structural, thermal and electrical properties of Li_{4-2x} Zn_xSiO_4 ceramic electrolyte prepared by citrate sol–gel technique, International Journal of Electrochemical Science 8 (2013) 6055–6067.